Chemical Science

ROYAL SOCIETY OF CHEMISTRY

EDGE ARTICLE

View Article Online
View Journal | View Issue

Cite this: *Chem. Sci.*, 2020, **11**, 2006

All publication charges for this article have been paid for by the Royal Society of Chemistry

The importance of the counter-cation in reductive rare-earth metal chemistry: 18-crown-6 instead of 2,2,2-cryptand allows isolation of $[Y^{II}(NR_2)_3]^{1-}$ and ynediolate and enediolate complexes from CO reactions†

Austin J. Ryan, Joseph W. Ziller and William J. Evans *

The use of 18-crown-6 (18-c-6) in place of 2.2.2-cryptand (crypt) in rare earth amide reduction reactions involving potassium has proven to be crucial in the synthesis of Ln(II) complexes and isolation of their CO reduction products. The faster speed of crystallization with 18-c-6 appears to be important. Previous studies have shown that reduction of the trivalent amide complexes $Ln(NR_2)_3$ (R = $SiMe_3$) with potassium in the presence of 2.2.2-cryptand (crypt) forms the divalent $[K(crypt)][Ln^{II}(NR_2)_3]$ complexes for Ln = Gd, Tb, Dy, and Tm. However, for Ho and Er, the $[Ln(NR_2)_3]^{1-}$ anions were only isolable with $[Rb(crypt)]^{1+}$ counter-cations and isolation of the $[Y^{II}(NR_2)_3]^{1-}$ anion was not possible under any of these conditions. We now report that by changing the potassium chelator from crypt to 18-crown-6 (18-c-6), the $[Ln(NR_2)_3]^{1-}$ anions can be isolated not only for Ln = Gd, Tb, Dy, and Tm, but also for Ho, Er, and Y. Specifically, these anions are isolated as salts of a 1 : 2 potassium : crown sandwich cation, $[K(18\text{-c-}6)_2]^{1+}$, *i.e.* $[K(18\text{-c-}6)_2][Ln(NR_2)_3]$. The $[K(18\text{-c-}6)_2]^{1+}$ counter-cation was superior not only in the synthesis, but it also allowed the isolation of crystallographically-characterizable products from reactions of CO with the $[Ln(NR_2)_3]^{1-}$ anions that were not obtainable from the $[K(crypt)]^{1+}$ analogs. Reaction of CO with $[K(18\text{-c-}6)_2][Ln(NR_2)_3]$, generated *in situ*, yielded crystals of the ynediolate products, $\{[(R_2N)_3Ln]_2(\mu\text{-}OC{\equiv}CO)\}^{2-}$, which crystallized with counter-cations possessing 2 : 3 potassium : crown ratios, *i.e.*$\{[K_2(18\text{-c-}6)_3]\}^{2+}$, for Gd, Dy, Ho. In contrast, reaction of CO with a solution of isolated $[K(18\text{-c-}6)_2][Gd(NR_2)_3]$, produced crystals of an enediolate complex isolated with a counter-cation with a 2 : 2 potassium : crown ratio namely $[K(18\text{-c-}6)]_2^{2+}$ in the complex $[K(18\text{-c-}6)]_2\{[(R_2N)_2Gd_2(\mu\text{-}OCH{=}CHO)_2]\}$.

Received 15th November 2019
Accepted 4th January 2020

DOI: 10.1039/c9sc05794c

rsc.li/chemical-science

Introduction

Reductive rare earth chemistry has undergone major changes in the past twenty years. Since complexes of Eu(II), Yb(II), and Sm(II) were discovered around 1906, it was believed that these were the only +2 lanthanide ions accessible in molecular complexes up until 1997. The discovery of molecular complexes of Tm(II), Dy(II), and Nd(II) in 1997–2001 changed that view.[1–4] The discovery of La(II) and Ce(II) complexes by Lappert in 2008 (ref. 5) showed that the early lanthanides could also form Ln(II) complexes. Studies of dinitrogen reduction subsequently led to the discovery of molecular Ln(II) complexes for all of the lanthanides and yttrium.[6–8]

In 2011, as part of an investigation of LnA_3/M reactions (Ln = rare-earth metal; A = anion; M = alkali metal) related to the reduction of dinitrogen which provided $(N_2)^{2-}$ and $(N_2)^{3-}$ complexes,[9–14] evidence for an Y(II) ion in solution was reported based on an EPR spectrum of the product obtained from treatment of $Y(NR_2)_3$ (R = $SiMe_3$) with K in THF at −35 °C under argon.[15] Although the two-line spectrum arising from the ^{89}Y I = 1/2 nucleus indicated the presence of Y(II), structural confirmation of an Y(II) amide complex was elusive. By switching from bis(silyl)amide ancillary ligands to the silylcyclopentadienyl ligand, $C_5H_4SiMe_3$ (Cp′), a crystallographically characterizable Y(II) complex was isolated by reduction of Cp'_3Y with KC_8 in the presence of 18-crown-6 (18-c-6), namely $[K(18\text{-c-}6)][YCp'_3]$, eqn (1).[6]

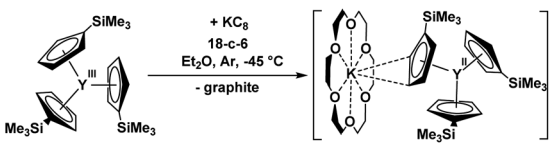

(1)

Department of Chemistry, University of California, Irvine, California 92697-2025, USA. E-mail: wevans@uci.edu

† Electronic supplementary information (ESI) available. CCDC 1950288–1950300. For ESI and crystallographic data in CIF or other electronic format see DOI: 10.1039/c9sc05794c

Subsequently, it was found that the 2.2.2-cryptand (crypt) chelate allowed isolation of a more stable form of the $(Cp'_3Y)^{1-}$ anion in the complex, [K(crypt)][YCp'_3].[8] The crypt chelate proved to be effective in isolating [K(crypt)][$LnCp'_3$] complexes for all the lanthanide metals except radioactive *Pm*, eqn (2).[6–8,16] Crypt was also effective in stabilizing Ln(II) ions of La and Ce in earlier seminal studies of M. F. Lappert and coworkers using the $C_5H_3(SiMe_3)_2$ (Cp″) ligand,[5] and this was extended to Pr and Nd as well, eqn (2).[17] These results showed that LnA_3/K reactions with A = silylcyclopentadienyl ligands, when done in the presence of crypt, could provide Ln(II) complexes across the series.[3,4]

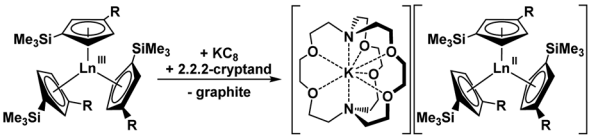

(2)

An explanation for the efficacy of the silylcyclopentadienyl ligands was possible from the hyperfine coupling constants of the EPR spectra of the yttrium complexes. The hyperfine coupling constant of the $Y(NR_2)_3$/K reduction product, 110 Gauss,[15] was considerably larger than the 36.6 Gauss coupling constant of (Cp'_3Y)[1–6] and suggested that more of the unpaired electron density was located on the metal in the amide complex. It was reasoned that this was the cause of its limited stability and made it too reactive to isolate. Since trivalent complexes of yttrium and lanthanides of similar size, particularly Ho and Er, have always displayed similar chemistry, it was assumed the $[Ln(NR_2)_3]^{1-}$ complexes could not be isolated either.

It was therefore surprising that alkali metal reduction of $Sc(NR_2)_3$ in the presence of both 18-c-6 and crypt generated crystallographically-characterizable Sc(II) complexes, $[Sc(NR_2)_3]^{1-}$, eqn (3).[18] This indicated that scandium displayed different chemistry from the yttrium congener directly below it in the periodic table.

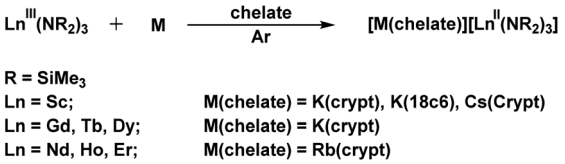

(3)

This suggested that the yttrium/late lanthanide comparison should be re-evaluated. Surprisingly, it was found that reduction of the $Ln(NR_2)_3$ complexes of Gd, Tb, and Dy with K in the presence of crypt generated crystallographically-characterizable Ln(II) complexes, [K(crypt)][$Ln(NR_2)_3$], **1-Ln**, like Sc.[19] Hence, these rare-earth metals also differed from yttrium. For Ln = Nd, Ho and Er, however, it was necessary to use Rb as the reductant in the presence of crypt to obtain crystals of the $[Ln(NR_2)_3]^{1-}$ anions as [Rb(crypt)][$Ln(NR_2)_3$]. Attempts to isolate either salt of the yttrium anion, $[Y(NR_2)_3]^{1-}$, were unsuccessful.

Although an Y(II) complex was not yet isolated with amide ligands, the reactivity of the $Y(NR_2)_3$/K system was explored with CO and led to complexes of $(CO)^{1-}$ and $(OC{\equiv}CO)^{2-}$, eqn (4).[20]

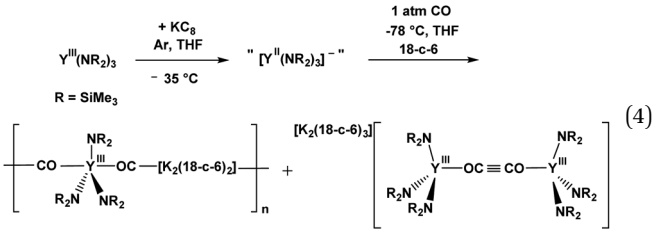

(4)

We now report that by switching from crypt as the potassium chelator to two equivalents of 18-c-6 in the reduction protocol for rare earth $Ln(NR_2)_3$ complexes, not only can Ln(II) complexes of Ho and Er be isolated with K as the reductant, but the $[Y(NR_2)_3]^{1-}$ anion, elusive since 2011, can be isolated and crystallographically characterized. These results were unexpected since the $(YCp'_3)^{1-}$ anion is more stable with crypt as a potassium chelate compared to 18-c-6 and in this study none of the cations are near the anions in the solid state. Stability studies on the 18-c-6 complexes suggest that the speed of crystallization is a critical factor. In addition, we describe how these $[K(18\text{-c-}6)_2]^{1+}$ salts enhance the reaction chemistry of the new Ln(II) complexes by allowing isolation of CO reduction products not obtainable from the $[K(crypt)]^{1+}$ analogs. New ynediolate complexes and an unusual enediolate complex derived from CO reduction and homologation are presented as further examples of the importance of the potassium chelating agent in these rare-earth metal reduction systems.

Results

Synthesis

Gd, Tb, Dy. Initially, potassium graphite reduction of $Tb(NR_2)_3$ (R = $SiMe_3$) was performed with a 1 : 1 ratio of $Tb(NR_2)_3$ to 18-crown-6 (18-c-6) to evaluate the necessity of the 2.2.2-cryptand (crypt) chelate in isolating the Ln(II) species. Upon reduction, a deep blue solution was produced similar to that of [K(crypt)][$Tb(NR_2)_3$], **1-Tb**. Layering with hexanes yielded dark blue crystals. X-ray diffraction indicated that the $[Tb(NR_2)_3]^{1-}$ anion had formed, but, surprisingly, there were two 18-c-6 units per potassium in the counter-cation: $[K(18\text{-c-}6)_2][Tb(NR_2)_3]$, **2-Tb**, Fig. 1. Subsequent reductions were then performed with a 1 : 2 ratio of $Ln(NR_2)_3$ to 18-c-6 which led to an increased yield, 75%. The same reaction conditions were applied to $Gd(NR_2)_3$ and $Dy(NR_2)_3$ and the analogous complexes, **2-Gd** and **2-Dy**, were isolated in similar yields, eqn (5).

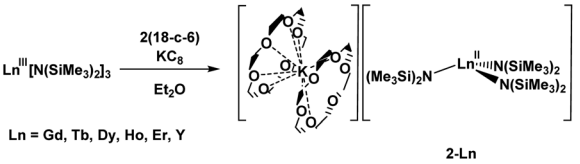

(5)

Ho, Er, Tm. Given the success of the reaction above, the protocol was extended to Er and Ho which had previously produced crystals of the $[Ln(NR_2)_3]^{1-}$ anions only with the $[Rb(crypt)]^{1+}$ cation. Crystallographically-characterizable complexes of Ho and Er were also obtainable with K as the reductant using 18-c-6 according to eqn (5).

This synthesis was also examined with Tm, a metal that forms Ln(II) complexes with traditional $4f^{n+1}$ electron configurations in contrast to the metals above that form $4f^n5d^1$ ions.[3,4,7,8,16] This reaction was also successful and provided $[K(18\text{-c-}6)_2][Tm(NR_2)_3]$, **2-Tm**.

Yttrium. Given the success of the 18-c-6 protocol observed with the lanthanides, attempts were again made using this chelate in the reduction of $Y(NR_2)_3$. Initial reductions were performed as shown in eqn (4) leading to the crystallization of the complex $[K(18\text{-c-}6)_2][Y(NR_2)_3]$, **2-Y**, as determined by X-ray diffraction. Subsequent attempts to synthesize **2-Y** revealed that a temperature of −78 °C helped to avoid significant decomposition of **2-Y** during the synthesis. The EPR spectrum of **2-Y** is indistinguishable from that of the $Y(NR_2)_3$/K reduction product reported in 2011.[15]

Structure

The **2-Ln** complexes of Ln = Gd, Tb, Dy, Ho, Er, and Y, Fig. 1, are isomorphous and crystallize in the $P2_1/n$ space group. The crypt analogs also formed an isomorphous series, **1-Ln**, for Ln = Gd, Tb, and Dy, and these were also isomorphous with the analogs containing Rb cations, $[Rb(crypt)][Ln(NR_2)_3]$, **1-Ln(Rb)** for Ln = Ho, Er. These all crystallized in the space group $P\bar{1}$. The **2-Tm** complex is not isomorphous with the other **2-Ln** structures and crystallizes with two formula units per unit cell in the space group $P2_12_12_1$ (see ESI†).

$Ln(NR_2)_3$ and $[Ln(NR_2)_3]^{1-}$ complexes often show disorder in the position of the metal with respect to the plane of the three nitrogen donor atoms. The $Ln(NR_2)_3$ complexes of Nd,[21] Eu,[22] Tb,[23] Dy,[24] Er,[24] Yb,[25] and Lu[26] exhibit disorder of the metal about an inversion center such that the metal is located above and below the N_3 plane in the range of 0.34–0.58 Å. In **1-Gd**, **1-Tb**, **1-Dy**, and **1-Ho(Rb)**, the metals are disordered 0.5–0.6 Å above and below the plane with disorder in the 65–75% range.[19] It should be noted that this disorder depends on reaction and crystallization conditions. For example, **1-Gd**, synthesized in THF and crystallized from THF/hexane formed crystals in the $P\bar{1}$ space group and showed the disorder mentioned above.[17] However, a sample synthesized for this study in Et_2O/toluene and crystallized by layering with hexanes formed crystals in the trigonal space group $R3$ with no disorder. The structure had an asymmetric unit consisting of one amide ligand on Gd and a potassium cation with one third of crypt chelate. Unfortunately, the data on this new structure were not of high enough quality to discuss bond lengths (see ESI†). The disorder in the structures of both $Sc(NR_2)_3$ and $[Sc(NR_2)_3]^{1-}$ was found to be highly dependent on the crystallization conditions.[18]

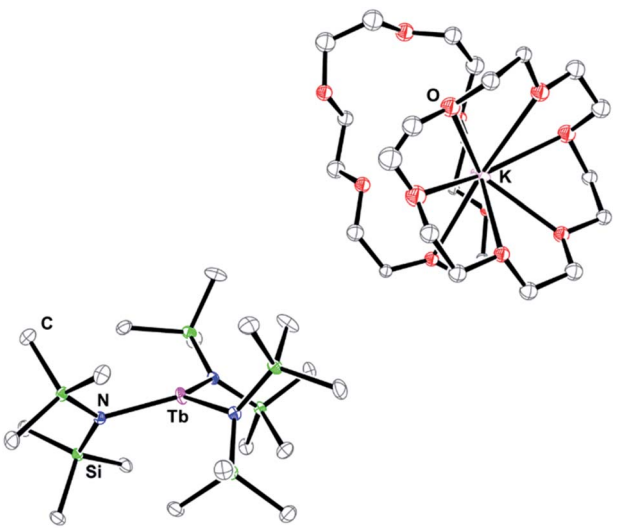

Fig. 1 Thermal ellipsoid plot of **2-Tb** drawn at the 50% probability level. Hydrogen atoms and disordered 18-c-6 atoms are excluded for clarity. The other **2-Ln** complexes (Ln = Gd, Tb, Dy, Ho, Y, Er) are all isomorphous.

In comparison, the crystallographic data on **2-Gd**, **2-Tb**, and **2-Tm** were successfully modeled without a disordered metal center. These complexes had trigonal pyramidal structures with the metal out of the plane by 0.055–0.201 Å (see below). The data on **2-Dy**, **2-Ho**, **2-Er**, and **2-Y** were best modeled with only minor disorder of the metal where 97% of the metal lies above and close to the N_3 plane (within 0.283 Å) and 3% lies below the plane by 0.554 Å.

Metrical data on **1-Ln** and **2-Ln** are presented in Table 1. As shown, the structures of the $[Ln(NR_2)_3]^{1-}$ anions in **2-Ln** are identical within experimental error to the anions in **1-Ln** and **1-Ln(Rb)**. The parallels also apply to **1-Tm** and **2-Tm** which are assigned traditional $4f^{n+1}$ electron configurations. As has been found in other series of Ln(II) complexes,[3,4,16,19] different structural parameters are observed for complexes of $4f^{n+1}$ and $4f^n5d^1$ Ln(II) ions. Specifically, the metrical parameters of $[Tm(NR_2)_3]^{1-}$ in **1-Tm** and **2-Tm** have Tm–N distances longer than those in the $Tm(NR_2)_3$ starting material by 0.2 Å. For Gd, Tb, Dy, and Ho, the Ln–N distances are only 0.05 Å longer than in the $Ln(NR_2)_3$ starting materials suggesting that **2-Ln** for Ln = Gd, Tb, Dy and Ho, like those of **1-Ln**, are $4f^n5d^1$. Comparisons cannot be made

Table 1 Comparison of metal ligand distances (Å) of [K(crypt)][$Ln(NR_2)_3$], **1-Ln**, [Rb(crypt)][$Ln(NR_2)_3$], **1-Ln(Rb)**, [$K(18\text{-c-}6)_2$][$Ln(NR_2)_3$], **2-Ln**, and $Ln(NR_2)_3$

Metal	**1-Ln**, Ln–N avg	**2-Ln**, Ln–N avg	$Ln(NR_2)_3$, Ln–N avg	**1-Ln**, $Ln–N_{plane}$ avg	**2-Ln**, $Ln–N_{plane}$ avg
Gd	2.307	2.309	2.247[a]	0.523	0.158
Tb	2.282	2.293	2.233	0.503	0.201
Dy	2.270	2.280	2.213	0.523	0.436
Ho	2.256	2.267	2.211[a]	0.509	0.395
Er	—	2.249	2.210	NA	0.426
Tm	2.320	2.348	2.200[a]	0.023	0.055
Y	—	2.268	2.224	NA	0.418

[a] These three Ln(III) complexes do not have reported crystal structures, so expected Ln–N distances were interpolated from analogous complexes of metals with similar ionic radii.

for **1-Er(Rb)** since the reported structure was of low quality and provided connectivity only. Hence the structure of **2-Er** provided the first opportunity to evaluate this parameter with the $[Er(NR_2)_3]^{1-}$ anion. The data show a change in bond distance of 0.05 Å from Er(III)[24] to Er(II) consistent with a $4f^{11}5d^1$ electron configuration.

Spectroscopy

The UV-visible spectra of **2-Gd** and **2-Dy** are indistinguishable from those of **1-Gd** and **1-Dy** with strong, broad absorbances at 598 nm ($\varepsilon = 3500\ cm^{-1}\ M^{-1}$) and 608 nm ($\varepsilon = 1200\ cm^{-1}\ M^{-1}$). Spectra were also obtained for **2-Ho** and **2-Er** since $[Ln(NR_2)_3]^{1-}$ anions of these metals with crypt-based counter-cations were too unstable to provide optical data. These spectra also show strong absorbances around 600 nm ($\varepsilon = 3000$, 1800) similar to those reported for **1-Gd**, **1-Dy**, and **1-Tb**.[19] Interestingly, the spectrum for **2-Y** shows a strong absorbance at a longer wavelength, 650 nm ($\varepsilon = 3800$), than those of **1-Ln** and **2-Ln**. All of the spectra of the $[Ln(NR_2)_3]^{1-}$ complexes are shown in Fig. 2 (individual spectra are shown in the ESI†). The UV-visible spectra of **1-Tm** and **2-Tm** are not as intense, which is typical of $4f^{n+1}$ Ln(II) ions *vs.* $4f^n5d^1$ Ln(II) ions as seen previously with $(Cp'_3Ln)^{1-}$ complexes.[3,4]

Stability

The $[K(crypt)]^{1+}$ complexes, $[K(crypt)][Ln(NR_2)_3]$, **1-Ln**, showed a trend in solution stability of Tm ~ Gd ≫ Tb > Dy ≫ Ho, Er ≫ Nd.[19] The **2-Ln** complexes have similar stability to those of **1-Ln** and display a similar trend. For **2-Tm**, a half-life of one week was observed, whereas **2-Gd** had a half-life of about 2 days. For **2-Dy**, a compound with moderate stability in the series, the half-life is approximately 5 minutes in a solution of diethyl ether, whereas **1-Dy**, which is not very soluble in Et_2O, shows a 5 minute half-life in THF (ESI†). The **2-Y** complex is even less stable than the other **2-Ln** compounds showing complete decomposition within 10 seconds at room temperature, which is consistent with the difficulty in isolating it previously. Decomposition products were not isolated, but C–H bond activation of the methyl ligands of $[N(SiMe_3)_2]^{1-}$ ligands to form cyclometalates involving $[N(SiMe_3)(SiMe_2CH_2)]^{2-}$ ligands is a frequent degradation route for rare earth amide complexes.

The stability data indicate that although the 18-c-6 chelate is better than crypt for crystallizing the $[Ln(NR_2)_3]^{1-}$ anions, it does not provide measurably more stable complexes in solution. The advantage of the $[K(18\text{-c-}6)_2]^{1+}$ complexes over the $[K(crypt)]^{1+}$ analogs is in the rate of crystallization. The **1-Ln** complexes typically require over 24 hours to crystallize, whereas the **2-Ln** compounds crystallize over the span of 2–3 hours. The more rapid crystallization is the likely reason that these **2-Ln** species of Ho, Er, and Y can be isolated. They are so reactive in solution that prolonged crystallization times lead to decomposition.

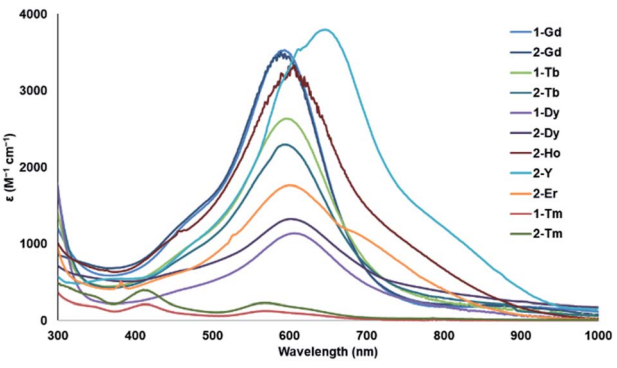

Fig. 2 UV-visible spectra of **1-Ln**[19] and **2-Ln**. Individual spectra and a table of absorption maxima and extinction coefficients are in the ESI.†

Reactivity with CO

Ynediolate formation. Previously, the $Y(NR_2)_3/K$ reaction conducted *in situ* without an isolated Y(II) complex under CO led to the CO reduction chemistry shown in eqn (3).[20] Attempts to explore this CO reduction chemistry with isolated complexes of the crypt chelate $[K(crypt)][Ln(NR_2)_3]$, **1-Ln**, for Ln = Gd and Dy did not lead to any crystallizable products. However, reactions of CO with the 18-c-6 chelate, $[K(18\text{-c-}6)_2][Ln(NR_2)_3]$, **2-Ln**, for Ln = Gd, Dy, and Ho did provide crystalline materials as described in the following paragraphs.

***In situ* reactions.** Due to the limited stability of **2-Ln** in solution, the starting complexes were generated *in situ* and used without isolation. Reductions of $Ln(NR_2)_3$ (Ln = Gd, Dy, Ho) were performed in Et_2O with KC_8 in an H-shaped tube equipped with greaseless high vacuum stopcocks (see ESI†) at −78 °C in the presence of 18-c-6. Introduction of CO gas at 1 atm to the system caused the dark blue solution to turn pale yellow immediately upon thawing. After the solution was allowed to warm to room temperature, pale yellow crystals of the CO-coupled ynediolate complex, $\{K_2(18\text{-c-}6)_3\}\{[(R_2N)_3Ln]_2(\mu\text{-}OC{\equiv}CO)\}$, **3-Ln** (Ln = Gd, Dy, Ho), had formed and could be isolated without further work-up, Fig. 3, eqn (6).

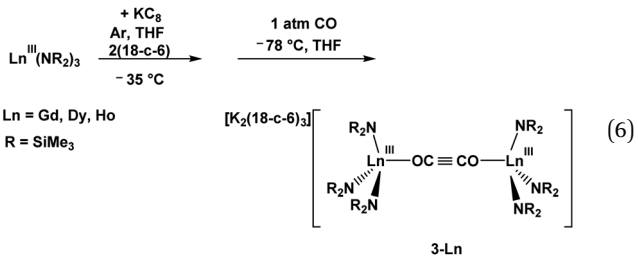

(6)

These **3-Ln** complexes were isomorphous with those previously reported for Y and Lu, eqn (3).[20] Hence, the ynediolate products generated in eqn (3) before any Y(II) and Lu(II) complexes had been identified, can also be formed from solutions containing established Ln(II) ions.

Only the metrical parameters for **3-Dy** and **3-Ho** can be compared with other complexes, since the crystal data on **3-Gd** were not of high enough quality for detailed analysis. As expected for isomorphous complexes, the 1.183(6)–1.186(4) Å

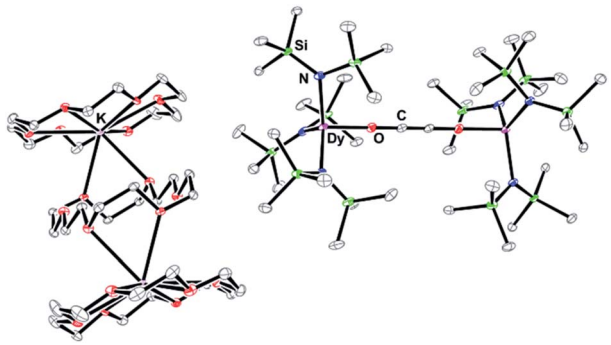

Fig. 3 Thermal ellipsoid plot of **3-Dy** (**3-Ln** are isomorphous) drawn at the 50% probability level. H atoms and lattice solvent molecules are excluded for clarity.

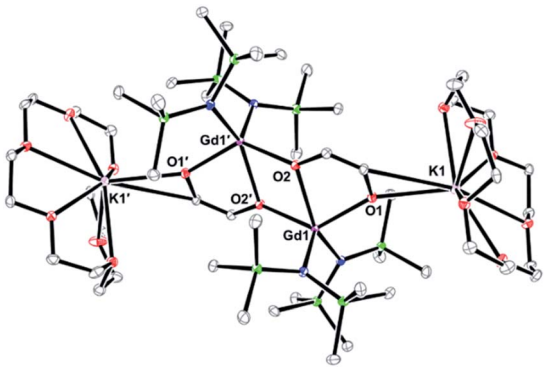

Fig. 4 Thermal ellipsoid plot of **4-Gd** drawn at the 50% probability level. H atoms and second molecule of **4-Gd** are omitted for clarity.

C≡C and 1.301(2)–1.311(4) Å C–O distances in **3-Dy** and **3-Ho** are very similar to those in **3-Y** and **3-Lu.** These distances also match other ynediolate complexes in the literature such as $[(A)_3U]_2(\mu\text{-OC}{\equiv}\text{CO})$ (A = $N(SiMe_3)_2$,[27] $OC_6H_2Bu^t_3$-2,4,6 (ref. 28)), $[U(Tren^{DMSB})]_2(\mu\text{-OC}{\equiv}\text{CO})$ [$Tren^{DMSB}$ = $N(CH_2CH_2NSiMe_2Bu^t)_3$],[29] and $[U(C_8H_6\{Si^iPr_3\text{-}1,4\}_2)(C_5Me_5)]_2(\mu\text{-OC}{\equiv}\text{CO})$.[30] The Ln–O distances vary as expected based on ionic radii:[31] 2.070(2) Å, Dy; 2.0598(14) Å, Ho; 2.057 Å, Y;[20] 2.021 Å, Lu.[20]

Reactions with isolated complexes

A thulium ynediolate. Interestingly, the Tm(II) complex, **2-Tm**, can also form an isomorphous ynediolate product. In this case, since the $4f^{13}$ **2-Tm** is more stable than the $4f^n5d^1$ **2-Ln** complexes, the reaction was carried out with isolated **2-Tm**. When isolated $[K(18\text{-c-}6)_2][Tm(NR_2)_3]$ is dissolved in Et_2O at −78 °C, a dark solution forms. Upon addition of CO, the solution quickly turns pale yellow. Upon warming to room temperature overnight, the ynediolate complex, $\{K_2(18\text{-c-}6)_3\}\{[(R_2N)_3Tm]_2(\mu\text{-OC}{\equiv}\text{CO})\}$, **3-Tm**, crystallizes and was found to have a structure isomorphous with those of **3-Gd**, **3-Dy**, and **3-Ho**, eqn (7).

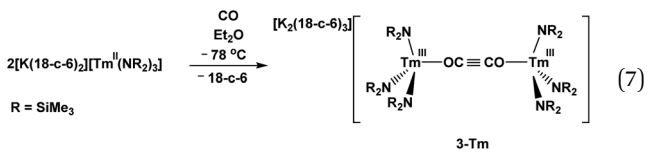

(7)

A gadolinium enediolate. Since $[K(18\text{-c-}6)_2][Ln(NR_2)_3]$, **2-Gd**, is the most stable $4f^n5d^1$ complex in the **2-Ln** series, a CO reaction with this complex in its isolated form was also examined. Solid **2-Gd** was added to one side of an H-tube with Et_2O stored at −78 °C on the other side. CO was then introduced to the system and the Et_2O was condensed onto **2-Gd** using a liquid nitrogen bath. The solution was then allowed to warm to −78 °C causing the solution to turn from dark blue to colorless. Concentration of the colorless solution produced a small amount of colorless crystals which were identified by X-ray diffraction as the enediolate complex $[K(18\text{-c-}6)]_2\{[(R_2N)_2Gd_2(\mu\text{-OCH}{=}\text{CHO})_2]\}$, **4-Gd**, eqn (8), Fig. 4. Hence, the CO reduction product that crystallized from this reaction is not the ynediolate of eqn (3), (6) and (7), but a derivative in which two hydrogen atoms per two metal centers have been added to what was presumed to be an ynediolate intermediate. In addition, one amide ligand has been lost per Gd metal center compared to the **2-Ln** precursor. The charge of the dianionic bimetallic complex is balanced by two $[K(18\text{-c-}6)]^{1+}$ units each of which is coordinated to an oxygen atom of an enediolate ligand. Although the origin of the additional hydrogen atoms in the enediolate in eqn (8) *versus* the **2-Ln** ynediolates is unknown and the yield is not synthetically useful, the reaction demonstrates the subtle differences that occur based on the reduction protocols.

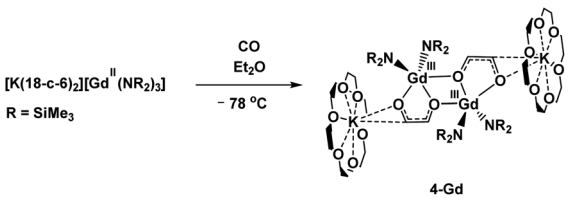

(8)

Enediolate complexes of f-elements have previously been obtained from reactions of lanthanide hydride[32,33] or tris(pentamethylcyclopentadienyl)lanthanide[34,35] complexes with CO. Additionally, enediolate formation incorporating actinides has been observed by the reductive insertion of CO into actinide alkyl bonds as well as by insertion of a bridging ynediolate into the C–H bond of a silylmethyl group in the complex $\{[(R_2N)_3U]_2(\mu\text{-OC}{\equiv}\text{CO})\}$ (R = $SiMe_3$).[27]

There are two independent anions in the unit cell of **4-Gd**, but their metrical parameters are similar. For example, the C=C distances in **4-Gd** of 1.334(4) and 1.331(4) Å are consistent with the presence of a double bond.[36] Average bond distances and angles of **4-Gd** are summarized in Fig. 5 (full data are in the ESI†). The 1.372(5) Å average C–O distance involving the oxygen of the enediolate that bridges the two Gd centers (O2) is similar to the 1.352(1) Å C–O distance for the oxygen of the enediolate that bridges Gd and K centers (O1).

The 2.322(1) to 2.356(5) Å range of Gd–N distances is only slightly larger than the 2.289(5) Å Dy–N average distance in **3-Dy**

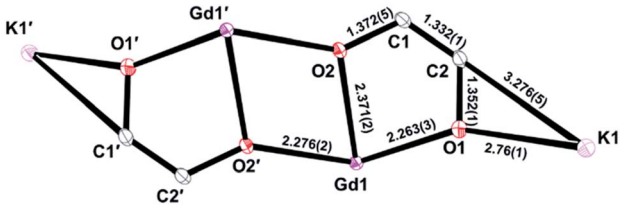

Fig. 5 Average bond distances (Å) of the two independent molecules in the unit cell for the core atoms of **4-Gd**.

although five coordinate Gd(III) is estimated to be 0.09 Å larger than 4-coordinate Dy(III) based on extrapolations of Shannon radii.[31] The interior Gd_2O_2 unit is rhombohedral rather than square with 2.371(2) Å Gd–O2 and 2.276(2) Å Gd–O2′ average Gd–O distances. The average 2.263(3) Gd–O1 distance is similar to the Gd–O2′ distance.

The 2.778(2) and 2.745(2) Å K–O(enediolate) distances are longer than the 2.669 Å K–O distance in $[Ta(OOO)(THF)]_2[Ta(OOO)H]_2[OC{=}C(O)C(O){=}C(O)\text{–}C(O){=}CO][K(DME)]_2$ where $H_3(OOO)$ is 2,6-bis(3-^{t}Bu-5-Me-2-hydroxybenzyl)-4-^{t}Bu-phenol,[37] but the latter complex has four coordinate potassium, whereas the potassium is formally eight coordinate in **4-Gd**. The 3.271(3) and 3.282(3) Å distances between the potassium cations and carbon atoms on the enediolate are within the 3.046 to 3.305 Å range of K···C distances found for $[K(18\text{-c-}6)]^{1+}$ to unsaturated carbon atoms found in molecules such as $[K(18\text{-c-}6)][Al(NON^{Ar})(C_8H_8)]$ (NON^{Ar} = $[O(SiMe_2NAr)_2]^{2-}$, Ar = 2,6-^{i}Pr$_2$C$_6$H$_3$),[38] $[K(18\text{-c-}6)(\eta^5\text{-Pdl*})]$ (Pdl* = dimethylnopadienyl),[39] and $[K(18\text{-c-}6)][LnCp''_2(C_6H_6)]$.[40]

Discussion

Reductions of the trivalent $Ln(NR_2)_3$ complexes with KC_8 in the presence of two equivalents of 18-c-6 allow for the crystallization of the divalent products, $[K(18\text{-c-}6)_2][Ln(NR_2)_3]$, **2-Ln**, in a matter of 2–4 hours, eqn (5). In contrast, reductions of $Ln(NR_2)_3$ with K in the presence of crypt require over 24 h to crystallize to $[K(crypt)][Ln(NR_2)_3]$, **1-Ln**. It appears that the faster crystallization times of **2-Ln** allow for +2 ions of Ho, Er, and Y to be isolated as $[K(18\text{-c-}6)_2]^{1+}$ salts. The analogous reactions with crypt did not give isolable products presumably due to decomposition during the long crystallization process. While the **2-Ln** complexes do not appear to be any more stable in solution at room temperature than the **1-Ln** series, the increased crystallization speed of **2-Ln** compared to **1-Ln** is the determining factor in the isolation of the more reactive **2-Y**. Hence, this is an important way in which the counter-cation can affect the chemistry.

The data to date on stability of the $[Ln(NR_2)_3]^{1-}$ anions suggests that stability decreases with decreasing size of the metal starting with Gd as the most stable non-traditional ion for both the **1-Ln** and **2-Ln** series. This may be one reason why the Y(II) derivative was so elusive for so long. The trend of decreasing stability as the metal becomes smaller has also been observed for the $[(C_5H_4SiMe_3)_3Ln]^{1-}$ (ref. 16) and $[(C_5Me_4H)_3Ln]^{1-}$ (ref. 41) series of anions, but in those cases the largest lanthanides, La–Pr, form the most stable complexes. For the $[Ln(NR_2)_3]^{1-}$ anions, Gd is the most stable and examples with larger metals are less stable.

The presence of 18-c-6 chelated potassium counter-cations also proved crucial to isolating CO reduction products in reactions of **2-Ln** generated *in situ* according to eqn (6) and (7). Ynediolate products $\{K_2(18\text{-c-}6)_3\}\{[(R_2N)_3Ln]_2(\mu\text{-}OC{\equiv}CO)\}$ **3-Ln**, were isolable starting from **2-Ln** that could not be isolated from reactions with the crypt-containing complexes $[K(crypt)][Ln(NR_2)_3]$, **1-Ln**. This is not to say that CO does not form ynediolate products with **1-Ln**. Ynediolate formation could have occurred in **1-Ln** reactions, but no products could be isolated to confirm that result. Again, the identity of the counter-cation is important in obtaining isolable crystals before other decomposition reactions occur.

The fact that 4f^{13} **2-Tm** made an ynediolate product like the 4f^{n}5d^1 **2-Gd**, **2-Dy**, and **2-Ho** complexes indicates that this CO reductive homologation does not necessarily require a 4f^{n}5d^1 electron configuration. As described above, ynediolates have previously been made from 5f^3 U(III) precursors, so d electron character is not a requirement for this reaction.

The isolation of the enediolate complex, $[K(crown)]_2\{[(R_2N)_2Gd_2(\mu\text{-}OCH{=}CHO)_2]\}$, **4-Gd**, eqn (8), from the reaction of CO with isolated **2-Gd** highlights the importance of reaction conditions in generating crystalline products that can be identified by X-ray crystallography. This is essential for these highly paramagnetic complexes. The reaction of CO with **2-Gd** generated *in situ* resulted in the isolation of ynediolate, **3-Gd**, but the reaction starting with isolated **2-Gd** provided a different crystalline product. Presumably the high reactivity of isolated **2-Gd** allowed C–H bond activation reactions to occur during the CO reaction which led to the enediolate complexes although the common by-product $HN(SiMe_3)_2$ was not observed. C–H bond activation in Ln(II) complexes has been previously observed.[17,42–45] Clearly, the details of these rare earth reduction reactions are critical to the isolation of crystalline products.

Conclusion

The importance of the counter-cation in isolating Ln(II) complexes is shown by the fact that the elusive $[Y(NR_2)_3]^{1-}$ anion can be isolated by potassium reduction of $Y(NR_2)_3$ in the presence of 18-c-6, but not crypt. The $[K(18\text{-c-}6)_2][Ln(NR_2)_3]$, **2-Ln**, complexes of Ho and Er are also more readily isolable than their crypt analogs, $[K(crypt)][Ln(NR_2)_3]$, **1-Ln**, which could only be isolated using Rb as a reductant as $[Rb(crypt)][Ln(NR_2)_3]$, **1-Ln(Rb)**. Although the **2-Ln** species are not more stable in solution than **1-Ln** complexes, the fact that they crystallize faster allows the isolation of the more reactive species in the series. Controlling the speed of crystallization of highly reactive complexes is a major challenge in chemistry that is currently not understood. It is well known that this is important factor in studies of highly radioactive actinide complexes,[46–48] but it clearly is important for these highly reducing $[Ln(NR_2)_3]^{1-}$ anions as well.

The identity of the counter-cation also affects the ease of isolation of reaction products of the reactive Ln(II) complexes as

demonstrated by the CO reactions. Reactions of CO with $[Ln(NR_2)_3]^{1-}$ anions with $[K(18\text{-c-}6)_2]^{1+}$ cations gave isolable products not obtainable with $[K(crypt)]^{1+}$ salts. The 18-c-6 system has the additional advantage over crypt in that it can form potassium chelates with a variety of sizes, charges, and potassium to 18-c-6 ratios, *i.e.* $[K(18\text{-c-}6)(solvent)_x]^{1+}$ ($x = 0, 1, 2$), $[K(18\text{-c-}6)_2]^{1+}$, and $[K_2(18\text{-c-}6)_3]^{2+}$.

The difference in reactivity with isolated solids (eqn (8)) *versus in situ* generated Ln(II) (eqn (6)) reflects the importance of minor details in channeling the Ln(II) reactivity to crystalline products allowing for crystallographic characterization, which is a primary method of characterization for complexes of these highly paramagnetic lanthanide ions. Since the identity of the counter-cation can determine if a complex is isolable or not, the choice of can be critical in several ways for the reaction chemistry. It is clear that the counter-cations must be carefully considered in future rare-earth reductive chemistry.

Experimental details

All manipulations and syntheses described below were conducted with the rigorous exclusion of air and water using standard Schlenk line and glovebox techniques under an argon or dinitrogen atmosphere. Solvents were sparged with UHP argon and dried by passage through columns containing Q-5 and molecular sieves prior to use. Elemental analyses were conducted on a PerkinElmer 2400 Series II CHNS elemental analyzer. Infrared spectra were collected as thin films on either a Thermo Scientific Nicolet iS5 spectrophotometer with an iD5 ATR attachment or an Agilent Cary 630 equipped with a diamond ATR attachment. UV-visible spectra were collected on either a Varian Cary 50 or Agilent Cary 60 UV-visible spectrometer. Evans method measurements were carried out on Bruker GN500 spectrometer.[49] Anhydrous $LnCl_3$ (Ln = Y, Gd, Tb, Dy, Ho, Er, Tm),[50] $Ln(NR_2)_3$ (R = $SiMe_3$),[51] and KC_8 (ref. 52) were prepared according to literature procedures. 18-Crown-6 (Alfa Aesar) was sublimed before use. CO (99.99%) was purchased from Airgas and used without further purification.

$[K(18\text{-c-}6)_2][Y(NR_2)_3]$, 2-Y

In an argon-filled glovebox, $Y(NR_2)_3$ (40 mg, 0.07 mmol) was combined with 18-c-6 (37 mg, 0.14 mmol) in Et_2O (2 mL) and cooled to −78 °C in the glovebox cold well. The cold solution was added to a vial containing KC_8 (14 mg, 0.11 mmol) that had also been cooled to −78 °C and the mixture was allowed to sit for about 1 min in the glovebox cold well. The solution was filtered through a pipette fit with a glass wool filter and layered with −78 °C hexanes before storing in the cold well. After 4 h, dark blue crystals **2-Y** (42 mg, 52%) were obtained. UV-vis (Et_2O) λ_{max}, nm (ε, M^{-1} cm^{-1}): 600 (3300 shoulder), 650 (3800). IR: 2940m 2888m, 1474w, 1453w, 1351m, 1236s, 1105s, 987s, 961s, 868m, 821s, 775m, 751m, 710w, 689w, 660m, cm^{-1}. Anal. calcd for $C_{42}H_{102}N_3O_{12}Si_6KY$: C, 44.34; H, 9.04; N, 3.69. Found: C, 43.80; H, 8.61; N, 3.25.

$[K(18\text{-c-}6)_2][Gd(NR_2)_3]$, 2-Gd

In an argon-filled glovebox, $Gd(NR_2)_3$ (40 mg, 0.062 mmol) was combined with 2 equivalents of 18-c-6 (33 mg 0.1825 mmol) in Et_2O (2 mL) and cooled to −35 °C in the glovebox freezer. The cold solution was added to a vial containing potassium graphite (12 mg, 0.094 mmol) that had also been cooled to −35 °C and the mixture was allowed to react about one minute in the glovebox freezer. The solution was filtered through a pipette fit with a glass wool filter and layered with −35 °C hexanes before being replaced in the glovebox freezer affording crystals suitable for X-ray diffraction after about 2 h (57 mg, 75%). UV-vis (Et_2O) λ_{max}, nm (ε, M^{-1} cm^{-1}): 275 (3380 shoulder), 607 (1130). IR: 2945s, 2889s, 2817m, 2761w, 2730w, 2702w, 1958w, 1478m, 1458m, 1446m, 1390w, 1355s, 1298m, 1260s, 1238s, 1135s, 1107s, 1079s, 1041s, 987s, 951s, 933m, 870s, 827s, 770m, 751m, 712m, 693m, 663s, 600m cm^{-1}. Anal. calcd for $C_{42}H_{102}N_3O_{12}Si_6KGd$: C, 41.82; H, 8.52; N, 3.48. Found: C, 41.40; H, 8.37; N, 3.30.

$[K(18\text{-c-}6)_2][Tb(NR_2)_3]$, 2-Tb

As described for **2-Gd**, $Tb(NR_2)_3$ (60 mg, 0.094 mmol) and 18-c-6 (50 mg, 0.188 mmol) in Et_2O (2 mL) were reacted with KC_8 (18 mg, 0.146 mmol) to afford **2-Tb** as a dark blue crystalline solid. Single crystals suitable for X-ray diffraction were grown by layering a concentrated Et_2O solution with hexanes (71 mg, 63%). UV-vis (Et_2O) λ_{max}, nm (ε, M^{-1} cm^{-1}): 595 (2300). IR: 2942s, 2889s, 2817m, 2762w, 2730w, 2698w, 1478m, 1458m, 1446m, 1356s, 1299m, 1260s, 1237s, 1135s, 1107s, 1078s, 1059s, 992s, 952s, 933m, 869s, 827s, 770m, 752m, 713m, 691m, 663s, 600m cm^{-1}. Anal. calcd for $C_{42}H_{102}N_3O_{12}Si_6KTb$: C, 41.77; H, 8.51; N, 3.48. Found: C, 41.81; H, 8.53; N, 3.23.

$[K(18\text{-c-}6)_2][Dy(NR_2)_3]$, 2-Dy

As described for **2-Gd**, $Dy(NR_2)_3$ (60 mg, 0.094 mmol) and 18-c-6 (50 mg, 0.188 mmol) in Et_2O (2 mL) were treated with KC_8 (18 mg, 0.146 mmol) to afford **2-Dy** as a dark blue crystalline solid. Single crystals suitable for X-ray diffraction were grown by layering a concentrated Et_2O solution with hexanes (62 mg, 53%). UV-vis (Et_2O) λ_{max}, nm (ε, M^{-1} cm^{-1}): 607 (1130). IR: 2945m, 2887m, 1475w, 1455w, 1358m, 1241s, 1109s, 992s, 958m, 867s, 827s, 7767m, 753m, 712w, 687w, 670s, 607m cm^{-1}. Anal. calcd for $C_{42}H_{102}N_3O_{12}Si_6KDy$: C, 41.64; H, 8.49; N, 3.47. Found: C, 41.11; H, 8.98; N, 3.32.

$[K(18\text{-c-}6)_2][Ho(NR_2)_3]$, 2-Ho

As described for **2-Gd**, $Ho(NR_2)_3$ (60 mg, 0.093 mmol) and 18-c-6 (46 mg, 0.186) in Et_2O (2 mL) were treated with KC_8 (18 mg, 0.146 mmol) to afford **2-Ho** as a dark blue crystalline solid. Single crystals suitable for X-ray diffraction were grown by layering a concentrated Et_2O solution with hexanes (64 mg, 57%). UV-vis (Et_2O) λ_{max}, nm (ε, M^{-1} cm^{-1}): 600 (1745), 691 (1115 shoulder). IR: 2940m, 2876m, 1475w, 1452w, 1352m, 1297w, 1234m, 1103s, 980s, 864m, 825s, 778m, 752m, 690w, 660m cm^{-1}. Anal. calcd for $C_{42}H_{102}N_3O_{12}Si_6KHo$: C, 41.56; H, 8.47; N, 3.46. Found: C, 41.33; H, 8.82; N, 3.53.

$[K(18\text{-c-}6)_2][Er(NR_2)_3]$, 2-Er

As described for **2-Gd**, $Er(NR_2)_3$ (60 mg, 0.092 mmol) and 18-c-6 (49 mg, 0.185 mmol) in Et_2O (2 mL) were reacted with KC_8 to afford **2-Er** as a dark blue crystalline solid. Single crystals suitable for X-ray diffraction were grown by layering a concentrated Et_2O solution with hexanes (60 mg, 53%). UV-vis (Et_2O) λ_{max}, nm (ε, M^{-1} cm^{-1}): 600 (1745), 691 (1115 shoulder). IR: 2938m, 2893m, 1472w, 1450w, 1347m, 1238w, 1105s, 980s, 871m, 825s, 775m, 750m, 715w, 695w, 660m, 600m cm^{-1}. Anal. calcd for $C_{42}H_{102}N_3O_{12}Si_6KEr$: C, 41.48; H, 8.45; N, 3.46. Found: C, 41.04; H, 8.39; N, 3.51.

$[K(18\text{-c-}6)_2][Tm(NR_2)_3]$, 2-Tm

As described for **2-Gd**, $Tm(NR_2)_3$ and 18-c-6 in Et_2O (2 mL) were reacted with KC_8 to afford **2-Tm** as a blue-green crystalline solid. Single crystals suitable for X-ray diffraction were grown by layering a concentrated Et_2O solution with hexanes. UV-vis (Et_2O) λ_{max}, nm (ε, M^{-1} cm^{-1}): 415 (385), 565 (230). IR: 2937m, 2886m, 1472w, 1471w, 1452w, 1417w, 1351m, 1231m, 1106s, 1053s, 961m, 871m, 815s, 747m, 715w, 657m cm^{-1}. Anal. calcd for $C_{42}H_{102}N_3O_{12}Si_6KTm$: C, 41.48; H, 8.45; N, 3.46. Found: C, 41.04; H, 8.39; N, 3.51.

$[K_2(18\text{-c-}6)_3][(R_2N)_3Ho]_2(\mu\text{-OC}{\equiv}\text{CO})$, 3-Ho

In an argon filled glove box, an H-shaped tube fitted with a filter frit in the middle (see ESI†) was loaded with $Ho(NR_2)_3$ (100 mg, 0.147 mmol), 18-c-6 (59 mg, 0.221 mmol), and Et_2O on one side and KC_8 (30 mg, 0.221 mmol) on the other. The apparatus was brought outside of the glovebox and attached to a vacuum line. Both sides of the H-tube were cooled to −78 °C and the Et_2O solution was poured onto the KC_8 generating a dark blue color. The mixture was allowed to react for about 10 min before the solution was filtered away from any excess KC_8. The solution was then frozen in liquid nitrogen and CO gas was introduced. The solution was allowed to warm to −78 °C resulting in a color change to pale yellow. The solution was then allowed to warm to room temp overnight producing crystals of **3-Ho** (49 mg, 27%). IR: 2949m, 2894m, 1445w, 1398w, 1349w, 1239s, 1125m, 1065m, 971s, 860m, 823s, 770m, 751w, 673w, 656m cm^{-1}. Anal. calcd for $C_{74}H_{180}Ho_2K_2N_6O_{20}Si_{12}$: C, 40.05; H, 8.17; N, 3.79. Found: C, 40.49; H, 7.95; N, 3.67.

$[K_2(18\text{-c-}6)_3][(R_2N)_3Dy]_2(\mu\text{-OC}{\equiv}\text{CO})$, 3-Dy

3-Dy was synthesized in a manner analogous to that of **3-Ho** (53 mg 28%). IR: 2949m, 2894m, 1445w, 1398w, 1349w, 1239s, 1125m, 1065m, 971s, 860m, 823s, 770m, 751w, 673w, 656m cm^{-1}.

$[K_2(18\text{-c-}6)_3][(R_2N)_3Gd]_2(\mu\text{-OC}{\equiv}\text{CO})$, 3-Gd

3-Gd was synthesized in a manner analogous to that of **3-Ho** (50 mg, 27%). IR: 2947m, 2893m, 1493w, 1464w, 1444w, 1354w, 1332w, 1295w, 1238s, 1105s, 978s, 942m, 858m, 825s, 767m, 656m cm^{-1}. Anal. calcd for $C_{74}H_{180}Gd_2K_2N_6O_{20}Si_{12}$: C, 40.33; H, 8.23; N, 3.81. Found: C, 40.37; H, 8.20; N, 3.53. μ_{eff} = 14.5 μ_B (Evans method).

$[K_2(18\text{-c-}6)_3][(R_2N)_3Tm]_2(\mu\text{-OC}{\equiv}\text{CO})$, 3-Tm

In an argon filled glovebox, **2-Tm** (100 mg, 0.082 mmol) was loaded into one side of an H-shaped tube fitted with a glass frit in between the two arms. Et_2O was loaded into the other side and the apparatus was removed from the glovebox and attached to a high vacuum line. Both sides were frozen in liquid nitrogen and CO (1 atm) was introduced to the system. The Et_2O was condensed onto the solid **2-Tm**. The solution was allowed to warm to −78 °C whereupon the solution turned yellow. The solution was allowed to warm to room temperature overnight and crystals of **3-Tm** suitable for X-ray diffraction grew on the side (50 mg, 27%). IR: 2937m, 2872m, 1470w, 1452w, 1393w, 1351m, 1238m, 1104s, 975s, 866m, 821s, 772m, 751w, 698w, 660m cm^{-1}.

$[K(18\text{-c-}6)]_2[(R_2N)Gd]_2(OHC{=}CHO)_2$, 4-Gd

In an argon filled glovebox, an H-shaped tube was loaded with solid $[K(18\text{-c-}6)_2][Gd(NR_2)_3]$ on one side and Et_2O on the other. The H-tube was removed from the glovebox and attached to a vacuum line. The Et_2O was frozen with liquid nitrogen and the H-tube was filled with CO gas. Et_2O was then condensed onto the solid $[K(18\text{-c-}6)_2][Gd(NR_2)_3]$ and allowed to warm to −78 °C causing the solution to turn from dark blue to colorless. The solution was then allowed to warm to room temperature overnight and a small amount of colorless crystals of **4-Gd** were recovered.

Conflicts of interest

There are no conflicts to declare.

Acknowledgements

We thank the U. S. National Science Foundation (CHE-1855328) for support of this research and Professor A. S. Borovik for assistance with EPR and UV-vis spectroscopy.

Notes and references

1 M. N. Bochkarev, *Coord. Chem. Rev.*, 2004, **248**, 835–851.
2 F. Nief, in *Handbook on the Physics and Chemistry of Rare Earths*, Elsevier, 2010, vol. 40, pp. 241–300.
3 D. H. Woen and W. J. Evans, *Handbook on the Physics and Chemistry of Rare Earths*, 2016, vol. 50, pp. 337–394.
4 W. J. Evans, *Organometallics*, 2016, **35**, 3088–3100.
5 P. B. Hitchcock, M. F. Lappert, L. Maron and A. V. Protchenko, *Angew. Chem., Int. Ed.*, 2008, **47**, 1488–1491.
6 M. R. MacDonald, J. W. Ziller and W. J. Evans, *J. Am. Chem. Soc.*, 2011, **133**, 15914–15917.
7 M. R. MacDonald, J. E. Bates, M. E. Fieser, J. W. Ziller, F. Furche and W. J. Evans, *J. Am. Chem. Soc.*, 2012, **134**, 8420–8423.
8 M. R. MacDonald, J. E. Bates, J. W. Ziller, F. Furche and W. J. Evans, *J. Am. Chem. Soc.*, 2013, **135**, 9857–9868.
9 W. J. Evans and D. S. Lee, *Can. J. Chem.*, 2005, **83**, 375–384.

10 W. J. Evans, D. S. Lee, C. Lie and J. W. Ziller, *Angew. Chem., Int. Ed.*, 2004, **43**, 5517–5519.
11 W. J. Evans, D. S. Lee, D. B. Rego, J. M. Perotti, S. A. Kozimor, E. K. Moore and J. W. Ziller, *J. Am. Chem. Soc.*, 2004, **126**, 14574–14582.
12 W. J. Evans, D. S. Lee, J. W. Ziller and N. Kaltsoyannis, *J. Am. Chem. Soc.*, 2006, **128**, 14176–14184.
13 J. D. Rinehart, M. Fang, W. J. Evans and J. R. Long, *Nat. Chem.*, 2011, **3**, 538–542.
14 J. D. Rinehart, M. Fang, W. J. Evans and J. R. Long, *J. Am. Chem. Soc.*, 2011, **133**, 14236–14239.
15 M. Fang, D. S. Lee, J. W. Ziller, R. J. Doedens, J. E. Bates, F. Furche and W. J. Evans, *J. Am. Chem. Soc.*, 2011, **133**, 3784–3787.
16 M. E. Fieser, M. R. MacDonald, B. T. Krull, J. E. Bates, J. W. Ziller, F. Furche and W. J. Evans, *J. Am. Chem. Soc.*, 2015, **137**, 369–382.
17 C. T. Palumbo, L. E. Darago, C. J. Windorff, J. W. Ziller and W. J. Evans, *Organometallics*, 2018, **37**, 900–905.
18 D. H. Woen, G. P. Chen, J. W. Ziller, T. J. Boyle, F. Furche and W. J. Evans, *Angew. Chem., Int. Ed.*, 2017, **56**, 2050–2053.
19 A. J. Ryan, L. E. Darago, S. G. Balasubramani, G. P. Chen, J. W. Ziller, F. Furche, J. R. Long and W. J. Evans, *Chem.–Eur. J.*, 2018, **24**, 7702–7709.
20 M. Fang, J. H. Farnaby, J. W. Ziller, J. E. Bates, F. Furche and W. J. Evans, *J. Am. Chem. Soc.*, 2012, **134**, 6064–6067.
21 R. A. Andersen, D. H. Templeton and A. Zalkin, *Inorg. Chem.*, 1978, **17**, 2317–2319.
22 J. S. Ghotra, M. B. Hursthouse and A. J. Welch, *J. Chem. Soc., Chem. Commun.*, 1973, 669–670.
23 P. B. Hitchcock, A. G. Hulkes, M. F. Lappert and Z. Li, *Dalton Trans.*, 2004, 129–136.
24 A. Herrmann Wolfgang, R. Anwander, C. Munck Florian, W. Scherer, V. Dufaud, W. Huber Norbert and R. J. Artus Georg, *Journal*, 1994, **49**, 1789.
25 P. G. Eller, D. C. Bradley, M. B. Hursthouse and D. W. Meek, *Coord. Chem. Rev.*, 1977, **24**, 1–95.
26 G. Scarel, C. Wiemer, M. Fanciulli, I. L. Fedushkin, G. K. Fukin, G. A. Domrachev, Y. Lebedinskii, A. Zenkevich and G. Pavia, *Z. Anorg. Allg. Chem.*, 2007, **633**, 2097–2103.
27 P. L. Arnold, Z. R. Turner, R. M. Bellabarba and R. P. Tooze, *Chem. Sci.*, 2011, **2**, 77–79.
28 S. M. Mansell, N. Kaltsoyannis and P. L. Arnold, *J. Am. Chem. Soc.*, 2011, **133**, 9036–9051.
29 B. M. Gardner, J. C. Stewart, A. L. Davis, J. McMaster, W. Lewis, A. J. Blake and S. T. Liddle, *Proc. Natl. Acad. Sci. U. S. A.*, 2012, **109**, 9265.
30 A. S. Frey, F. G. N. Cloke, P. B. Hitchcock, I. J. Day, J. C. Green and G. Aitken, *J. Am. Chem. Soc.*, 2008, **130**, 13816–13817.
31 R. Shannon, *Acta Crystallogr., Sect. A: Cryst. Phys., Diffr., Theor. Gen. Crystallogr.*, 1976, **32**, 751–767.
32 W. J. Evans, J. W. Grate and R. J. Doedens, *J. Am. Chem. Soc.*, 1985, **107**, 1671–1679.
33 E. L. Werkema, L. Maron, O. Eisenstein and R. A. Andersen, *J. Am. Chem. Soc.*, 2007, **129**, 2529–2541.
34 W. J. Evans, K. J. Forrestal and J. W. Ziller, *J. Am. Chem. Soc.*, 1995, **117**, 12635–12636.
35 W. J. Evans, S. A. Kozimor, G. W. Nyce and J. W. Ziller, *J. Am. Chem. Soc.*, 2003, **125**, 13831–13835.
36 F. H. Allen, O. Kennard, D. G. Watson, L. Brammer, A. G. Orpen and R. Taylor, *J. Chem. Soc., Perkin Trans. 2*, 1987, S1–S19.
37 T. Watanabe, Y. Ishida, T. Matsuo and H. Kawaguchi, *J. Am. Chem. Soc.*, 2009, **131**, 3474–3475.
38 R. J. Schwamm, M. D. Anker, M. Lein and M. P. Coles, *Angew. Chem., Int. Ed.*, 2019, **58**, 1489–1493.
39 A. C. Fecker, A. Glöckner, C. G. Daniliuc, M. Freytag, P. G. Jones and M. D. Walter, *Organometallics*, 2013, **32**, 874–884.
40 M. C. Cassani, Y. K. Gun'ko, P. B. Hitchcock, M. F. Lappert and F. Laschi, *Organometallics*, 1999, **18**, 5539–5547.
41 T. F. Jenkins, D. H. Woen, L. N. Mohanam, J. W. Ziller, F. Furche and W. J. Evans, *Organometallics*, 2018, **37**, 3863–3873.
42 J. F. Corbey, D. H. Woen, C. T. Palumbo, M. E. Fieser, J. W. Ziller, F. Furche and W. J. Evans, *Organometallics*, 2015, **34**, 3909–3921.
43 F. Jaroschik, A. Momin, F. Nief, X. F. Le Goff, G. B. Deacon and P. C. Junk, *Angew. Chem.*, 2009, **121**, 1137–1141.
44 C. T. Palumbo, D. P. Halter, V. K. Voora, G. P. Chen, A. K. Chan, M. E. Fieser, J. W. Ziller, W. Hieringer, F. Furche and K. Meyer, *Inorg. Chem.*, 2018, **57**, 2823–2833.
45 C. T. Palumbo, D. P. Halter, V. K. Voora, G. P. Chen, J. W. Ziller, M. Gembicky, A. L. Rheingold, F. Furche, K. Meyer and W. J. Evans, *Inorg. Chem.*, 2018, **57**, 12876–12884.
46 C. J. Windorff, G. P. Chen, J. N. Cross, W. J. Evans, F. Furche, A. J. Gaunt, M. T. Janicke, S. A. Kozimor and B. L. Scott, *J. Am. Chem. Soc.*, 2017, **139**, 3970–3973.
47 J. Su, C. J. Windorff, E. R. Batista, W. J. Evans, A. J. Gaunt, M. T. Janicke, S. A. Kozimor, B. L. Scott, D. H. Woen and P. Yang, *J. Am. Chem. Soc.*, 2018, **140**, 7425–7428.
48 C. A. P. Goodwin, J. Su, T. E. Albrecht-Schmitt, A. V. Blake, E. R. Batista, S. R. Daly, S. Dehnen, W. J. Evans, A. J. Gaunt, S. A. Kozimor, N. Lichtenberger, B. L. Scott and P. Yang, *Angew. Chem., Int. Ed.*, 2019, **58**, 11695–11699.
49 S. K. Sur, *J. Magn. Reson.*, 1989, **82**, 169–173.
50 M. D. Taylor, *Chem. Rev.*, 1962, **62**, 503–511.
51 D. C. Bradley, J. S. Ghotra and F. A. Hart, *J. Chem. Soc., Chem. Commun.*, 1972, 349–350.
52 D. E. Bergbreiter and J. M. Killough, *J. Am. Chem. Soc.*, 1978, **100**, 2126–2134.

